Supporting Information

Conductive nature of grain boundaries in nanocrystalline stabilized-Bi_2O_3 thin-film electrolyte

Seung Jin Jeong[1] , No Woo Kwak[1], Pilgyu Byeon[2], Sung-Yoon Chung[2] and WooChul Jung[1]*

[1]Department of MSE, Korea Advanced Institute of Science and Technology (KAIST), Daejeon 34141, Korea

[2]Graduate School of EEWS, Korea Advanced Institute of Science and Technology (KAIST), Daejeon 34141, Korea

Corresponding Author

*E-mail: wcjung@kaist.ac.kr (W.J.).

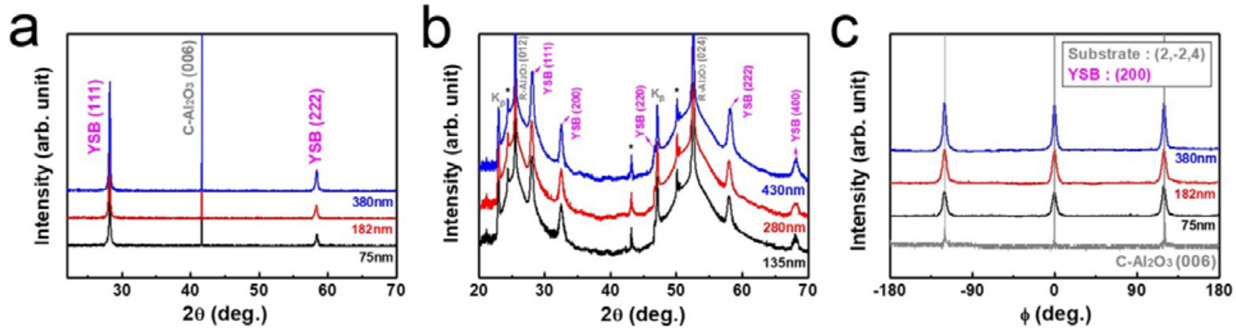

Figure S1. X-ray diffraction data for the Y-stabilized Bi_2O_3 thin films with different thicknesses. Out-of-plane diffraction patterns (2θ scan) of the films (a) on C-Al_2O_3 (0001) and (b) on R-Al_2O_3 $(1\bar{1}02)$. (c) In-plane diffraction patterns (φ scan) of the C-Al_2O_3 substrate and the YSB films.

Average grain size and grain boundary density measurement

In order to determine the average grain size and grain boundary densities, we drew a line with a fixed length (l) across the AFM image of each sample (Figure R9-a,b). The number of grain boundaries on the line was then counted (n) and the grain size (d = l/n) was determined (Figure R9-c,d). The grain boundary density was also obtained by counting the number of grain boundaries encountered per unit length (τ = n/l). This process was repeated with tens of different lines to obtain statistical values, while the length of the line was precisely held constant. This method is most common when measuring the grain size and grain boundary density. In addition, it should be noted that the grain size of the columnar thin film fabricated by the vacuum deposition process increases with the thickness. Because the density of the grain boundaries discussed in this study was obtained from surface AFM results, it represents the minimum density of the grain boundaries encountered during the actual oxygen ion conduction process.

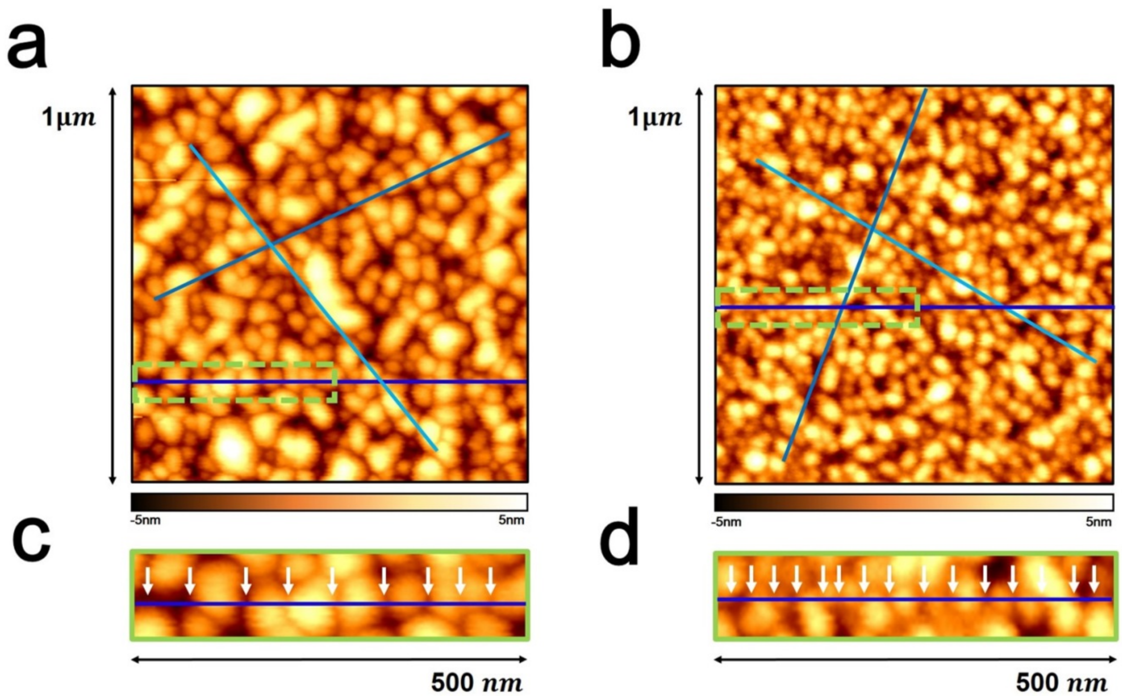

Figure S2. Examples illustrating the method used to calculate the average grain size and grain boundary density. (a), (b) Straight lines with a constant length were drawn across sample AFM images in a random direction. (c), (d) Magnified images of the green areas shown in (a) and (b).

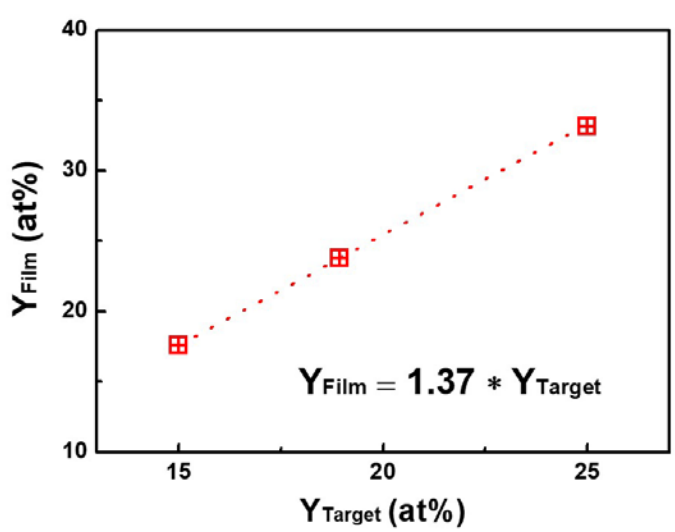

Figure S3. Chemical compositions of Y-stabilized Bi_2O_3 targets and thin films analyzed by inductively coupled plasma mass spectrometry (ICP-MS).

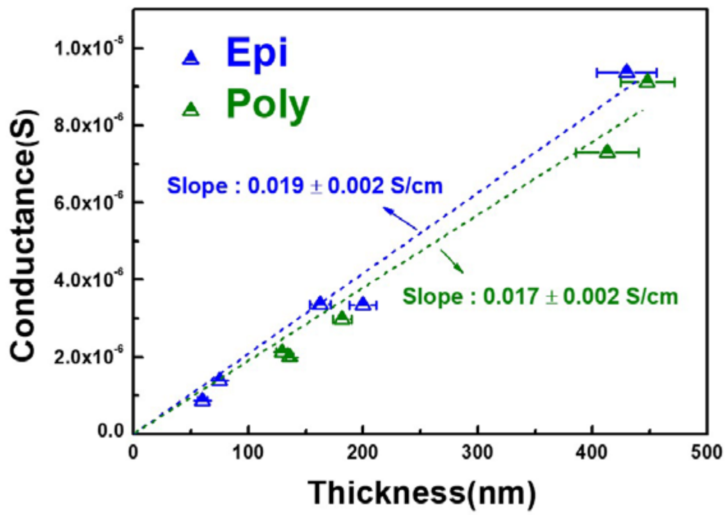

Figure S4. Conductance vs. thickness of the epitaxial (blue) and polycrystalline Y-stabilized Bi_2O_3 thin films.

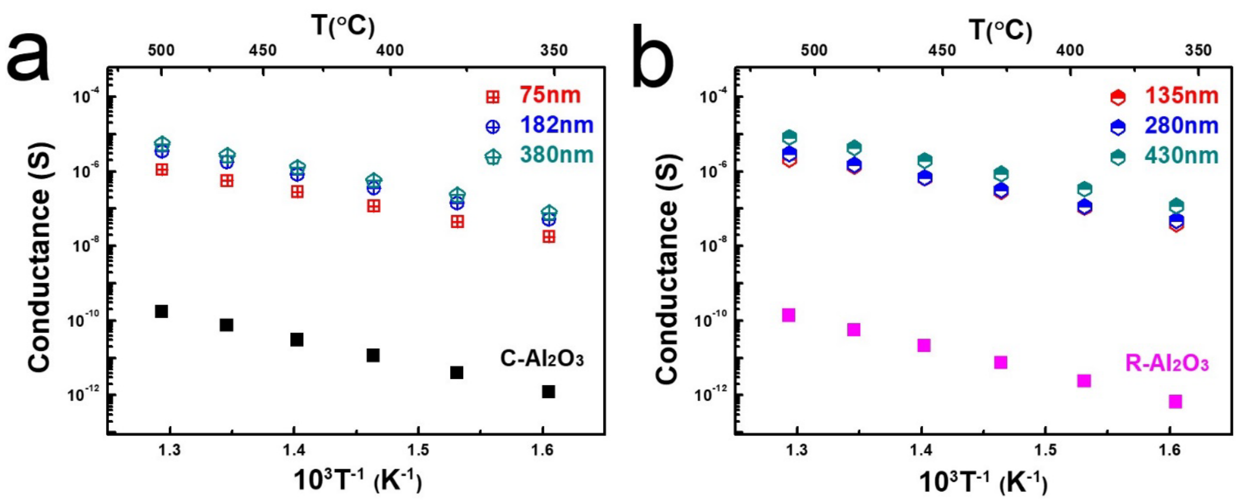

Figure S5. Conductance of (a) epitaxial Y-stabilized Bi_2O_3 thin films on C-Al_2O_3 and a bare C-Al_2O_3 substrate (black rectangle), and (b) columnar Y-stabilized Bi_2O_3 thin films on R-Al_2O_3 and a bare R-Al_2O_3 substrate (pink rectangle), respectively. The data were measured at temperatures between 350°C and 500°C and pO_2 = 0.21 atm.

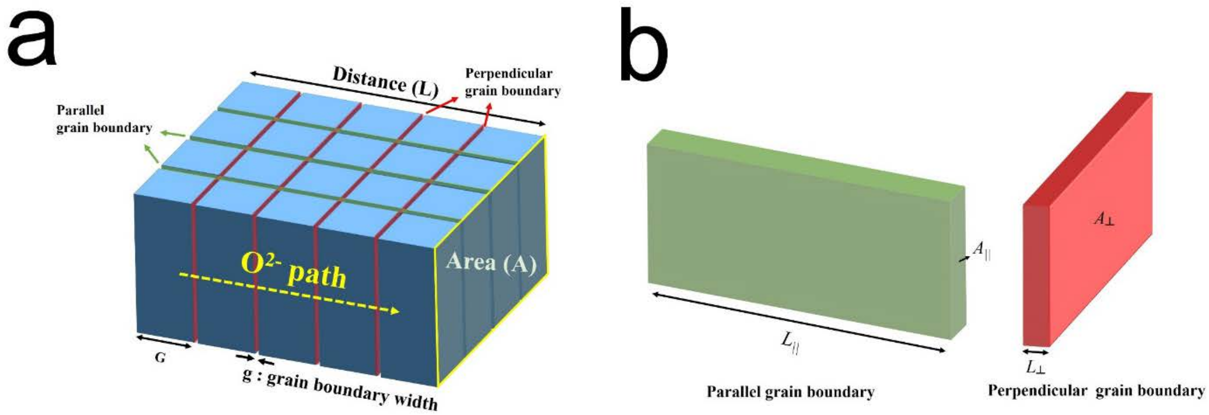

Figure S6. (a) Schematic of the "brick layer" model depicting the thin films used in this study, and (b) two regions, one in which oxygen ions are transported in a direction parallel to the grain boundaries and another in which they are transported perpendicular to the grain boundaries.

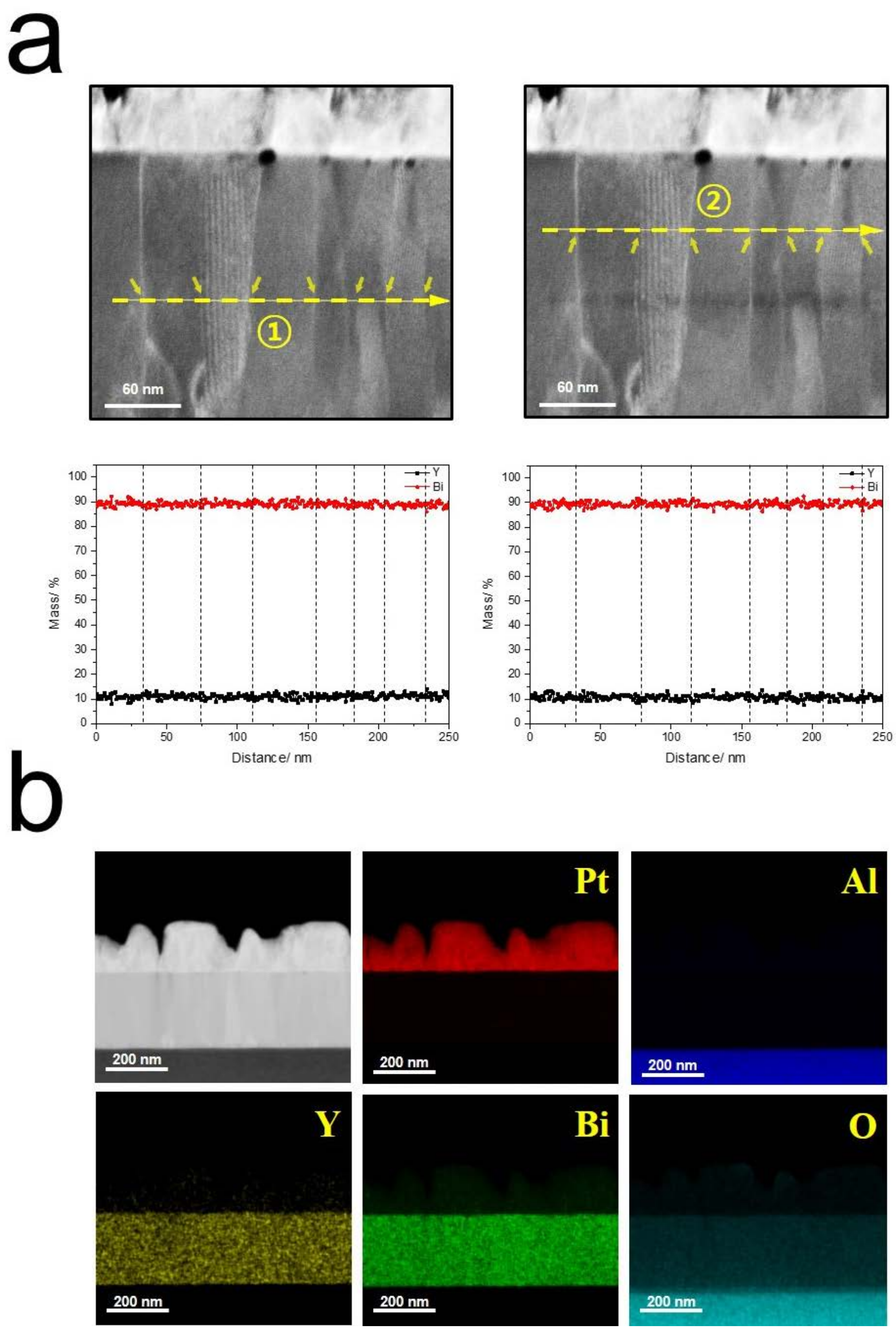

Figure S7. The additive compositional information obtained from HAADF-TEM images. (a) EDS compositional profiles of Y and Bi elements at different depths and (b) EDS mapping results, confirming no accumulation or segregation of specific components in vicinity of grain boundaries.